J. Obrzut, J. F. Douglas

National Institute of Standards and Technology, Polymers Division
Gaithersburg
USA
e-mail: jan.obrzut@nist.gov

MEASUREMENT OF COMPLEX CONDUCTIVITY IN CARBON NANOTUBE POLYMER COMPOSITES UNDER MECHANICAL SHEAR

We measured the complex conductivity of carbon nanotube-polypropylene composites under mechanical shear conditions. In order to determine how flow alters the properties of these complex fluids we constructed a rheo-dielectric test fixture, which allows for the simultaneous *in situ* measurement of both the frequency dependent complex electrical conductivity and basic rheological properties, such as shearing rate, viscosity, normal stresses. We analyzed the results using Generalized Effective Medium theory. The scaled conductivity of percolated networks compares well with the universal trend showing a power law scaling with frequency. We find that the conductivity percolation concentration (φ_c) increases with increasing shear rate. For sufficiently high shear rates, the nanocomposite undergoes a transition from a conducting to an insulating state. The shear rate dependence of φ_c, which gives rise to this transition, conforms well to a model that we introduced to describe this effect.

Keywords: complex conductivity, carbon nanotubes, percolation, composite materials, mechanical shear

1. INTRODUCTION

Carbon nanotubes have been studied as viable semiconductors, chemical sensors, and transparent cold conductive coatings. The attractive feature of these materials is that the addition of a relatively small amount of nanotubes into an insulating matrix can have a profound influence on the conductivity, optical and mechanical properties of the composite [1-3]. In our previous work, we showed that these materials exhibit unusual rheological and processing characteristics including shear thinning, negative normal stress, the suppression of the die swell and shear induced changes in the conductivity percolation [4]. In this paper, we describe a method to measure conductivity of melted carbon nanotube – polypropylene composites in well-defined flow fields as a function of shear rate and composition. Then, we discus the effect of shear on the

conductivity percolation threshold in the concentration regime where the conducting carbon nanotube network is most fragile.

2. METHODS

Composites containing multiwalled carbon nanotubes (CNT) [5, 6] in polypropylene (PP) were formed via melt blending [7]. Uniform dispersion containing 0.15%, 0.30% and 0.75% by volume of CNTs were obtained without surface functionalization of the tubes. The typical length of the dispersed tubes was about 10 μm and the diameter was about 50 nm. The rheo-dielectric experiments were performed using a rotational rheometer that was equipped with a dielectric test fixture shown in Fig. 1. The shearing plate of the test fixture contained conductive aluminum ring electrodes of width $w = 2$ mm and radius $r_1 = 4$ mm, $r_2 = 8$ mm and $r_3 = 12$ mm, separated by non-conductive polyamide regions. For a given rotational rate of the lower plate, the shear rate ($\dot{\gamma}$) increases radially as a function of position. This configuration allowed us to measure the conductivity at well-defined shear rates. The experiments were conducted at 190°C under a nitrogen atmosphere.
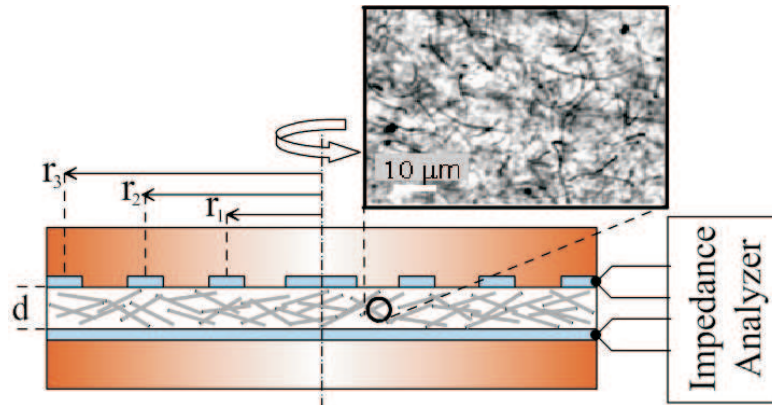

Fig. 1. Schematic representation of the test fixture. The surface of the shearing disk consists of aluminum electrode rings separated by an insulator. The microscopic image of the sheared sample is shown in the inset.

Complex impedance measurements (impedance magnitude $|Z^*|$ and the corresponding phase angle θ) of our CNT-PP composites were conducted in the frequency range of 40 Hz to 1 MHz through a four-terminal technique using an Agilent 4294A Precision Impedance Analyzer, calibrated with a standard extension adapter to Short, Load and Open standards. The complex conductivity, $\sigma^* = \sigma' + j\sigma''$, was obtained from the measured complex impedance, Z^*, normalized by the geometry of the test fixture:

$$\sigma^* = \frac{d}{Z^*(2\pi r \times w)}, \tag{1}$$

where d is the sample thickness, and the product of, r and w represents area of the ring electrode. These conductivity measurements were made in the *shear gradient* direction, i.e., perpendicular to flow streamlines.

The distinctive feature of the dielectric limit is $\sigma' \approx 0$, and a linear dependence of the imaginary conductivity (σ'') with frequency, while $\theta \approx -90°$. The lowest measurable conductivity in our system was $|\sigma^*| = |\sigma''| = 5 \times 10^{-9}$ S/m at 40 Hz, which is illustrated in Fig. 2b plot (7) for an air gap when the sample was removed. The upper measurement limit of the real conductivity was verified by bringing the two plates of the test fixture into contact in the absence of a sample, which resulted in $|Z^*|$ of $(1\pm0.1)\Omega$ and $\theta = (0 \pm 0.2)°$. For loss less dielectric materials θ is characteristically near $-90°$ while in the case of dielectrics with a loss due to intrinsic real conductivity, the phase angle between the AC voltage and the resulting current is in the range of $-90° \leq \theta < 0°$. The combined relative experimental uncertainty of the measured complex conductivity magnitude was within 2%, while the experimental uncertainty of the dielectric phase angle measurements was about $\pm0.5°$.

The complex conductivity of dielectric mixtures filled with conducting modifiers, such as CNT-PP, can be analyzed in terms of the resistance-capacitance ($R-C$) percolation model, in which the conducting and dielectric properties of the mix are represented by a network of idealized resistors R and capacitors with complex capacitance C^* [8, 9]. The equivalent complex admittance Y^* is the sum of the admittances of these two elements [7, 10].

$$Y^* = 1/R + j\omega C^*. \tag{2}$$

Accordingly, the complex conductivity, σ^*, of a specimen having thickness (d) and the active area of electrodes ($A = rw$) can be expressed by the equation (3).

$$\sigma^* = \sigma_0 + j\omega\varepsilon_0\varepsilon_r^*, \tag{3}$$

where $\omega = 2\pi f$ is again the angular frequency, ε_r^* is the complex relative dielectric permittivity of the material, $\varepsilon_r^* = \varepsilon_r' - j\varepsilon_r''$, ε_0 is the dielectric permittivity of free space, and $j^2 = -1$. Separating (3) into real and imaginary components we obtain:

$$\sigma' = \sigma_0 + \omega\varepsilon_0\varepsilon_r'', \tag{4}$$

and

$$\sigma'' = j\omega\varepsilon_0\varepsilon_r', \tag{5}$$

where σ_0 is frequency independent conductivity, $\omega = 2\pi f$ is the angular frequency, is the complex relative dielectric permittivity of the material, $\varepsilon_r^* = \varepsilon_r' - j\varepsilon_r''$, ε_0 is the dielectric permittivity of free space, and $j^2 = -1$. Thus, the scaling with frequency of

the in-phase component of the complex conductivity (σ') depends on the frequency dependence of $\varepsilon_r''(\omega)$, while the frequency dependence of the real part of the dielectric permittivity $\varepsilon_r'(\omega)$ determines the scaling of σ'' with frequency.

3. RESULTS AND DISCUSSION

Fig. 2 shows an example of the frequency dependent complex conductivity as a function of shear rate at 190°C for the CNTs concentration $\varphi = 0.18\%$ by volume. The general trend is that conductivity decreases with increasing shear rate. The real part (σ') of the complex conductivity exhibits a plateau at low frequencies, σ_0, (Fig. 2a), that persists up to the crossover frequency of ω_s. The plateau in the conductivity at $\omega < \omega_s$ indicates the existence of one or more percolation paths of real resistive elements R across the network that comprise an infinite cluster. We determined σ_0 values by fitting the experimental σ' data to equation (4) using a nonlinear least squares fitting routine. Our highest σ_0 values are in the range of about 0.01 S/m for CNT concentration of 0.75% by volume at lowest shear rates, comparable with results reported for similar composites [11]. The dipolar and carrier polarization, expressed by the real part of the dielectric permittivity (ε_r'), contribute primarily to σ''. The imaginary part σ'' of the complex conductivity is shown in Fig. 2b , where the slope of the plots corresponds to the real part (ε_r') of the complex dielectric permittivity (Eq. 5). The dashed straight lines represent σ'' calculated as a reference for several constant values of ε_r'. Fig. 2b demonstrates that the measured σ'' deviates from linearity, especially at higher frequencies, indicating that the composites exhibit not only frequency dependent conduction, but also that the dielectric polarization and dispersion are frequency dependent. Depending on the CNT concentration and shear rate, ε_r' can change by several orders of magnitude. In the case of a larger CNT concentration ($\varphi = 0.75\%$) and small shear rates, ε_r' approaches a value of about 10^4. With decreasing CNT concentration and increasing shear rate ε_r' decreases to about 10^3 (Fig. 2b, plot (1)), and eventually approaches the dielectric limit of the polymer matrix (PP), about 4.5 (see Fig. 2b. plots 6 and 7).

The crossover frequency, ω_s, corresponds to the macroscopic relaxation frequency that is related to the peak frequency of the dielectric loss. Above ω_s, in the multiple hopping regime, $\omega_s < \omega < \omega_0$, where ω_0 is the microscopic cut-off frequency, conduction occurs in the isolated clusters of sites and the real part of the conductivity increases with ω [12, 13]. Since ω_s depends on the distribution of the hopping conductivity sites in disordered materials i. e., it reflects the resistance between hopping sites and effective capacitance, it should scale accordingly with the dielectric permittivity [10, 14].

$$\omega_s \approx \sigma_0/(\varepsilon_0|\varepsilon_r^*|)_\omega. \tag{6}$$

We observe that ω_s increases with increasing σ_0, while it decreases when the dielectric permittivity increases. These two opposite trends are illustrated in Fig. 1.
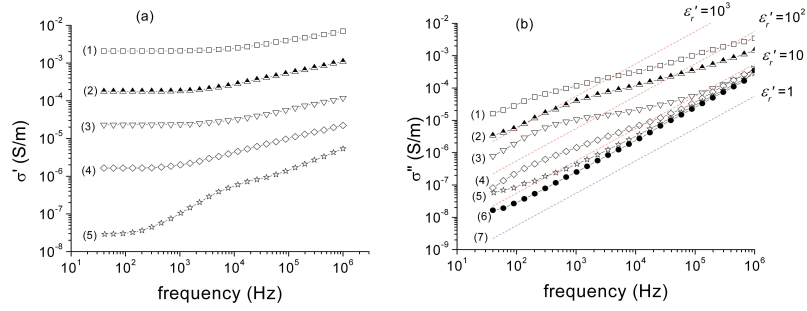
Fig. 2. (a) Real part σ', and (b) imaginary part σ'', of complex conductivity as a function of frequency for $\varphi = 0.15\%$ by volume of CNT in PP measured at the following shear rates: (1)-10^{-3} s^{-1}, (2)-0.2 s^{-1}, (3)-0.6 s^{-1}, (4)-1.0 s^{-1}, (5)-1.6 s^{-1} and (6)-3.0 s^{-1}. (7)- conductivity of an air gap when the sample was removed. The dashed straight lines in Fig. 2b represent σ'' calculated as a reference for constant ε_r' values of 1, 10, 100 and 1000 respectively.

For example, $\omega_s/2\pi$ is about 27 kHz in Fig. 2a plot (1), σ_0 is about 2.0×10^{-3} S/m, and $|\varepsilon_r^*|$ is about 1.4×10^3. Fig. 3 shows the conductivity results scaled as $\sigma'(\omega)/\sigma_0$ according to [14] with ω_s obtained by solving iteratively Eq. 6 against $\varepsilon_r'(\omega)$ and $\varepsilon_r''(\omega)$.
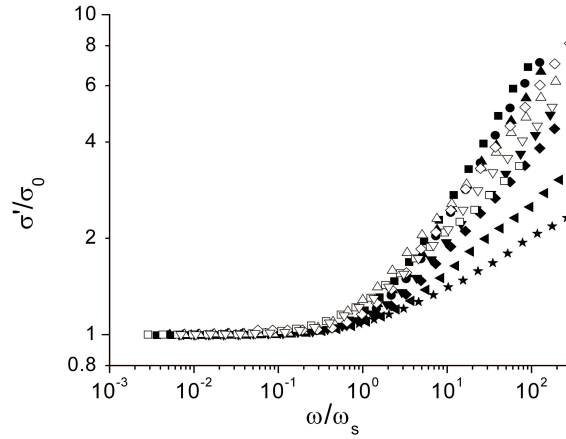

Fig. 3. Scaled conductivity (σ'/σ_0) vs. scaled frequency (ω/ω_s) for $\varphi = 0.3\%$ by volume (open symbols) and $\varphi = 0.75\%$ by volume (closed symbols) at different shear rates: 10^{-3} s^{-1}(squares) 0.2 s^{-1}(circles), 0.6 s^{-1}(triangles-up), 1.0 s^{-1}(triangles-down), 1.6 s^{-1}(diamonds), 3.0 s^{-1}a(tilt-triangles) and 6.3 s^{-1}(stars).

The scaled conductivity for percolated networks ($\phi > \phi_c$) compares well with the universal trend showing power law behavior ($\sigma' \sim \omega^n$) at $\omega > \omega_s$. The value of n in Fig. 3 is about 0.4 for all percolated networks when $\dot{\gamma} < 1$ s^{-1}. With increasing shear rate and decreasing CNT concentration, the exponent n decreases continuously,

approaching a value of about 0.12. The decreasing value of n indicates that the fraction of resistive paths decreases with shearing in favor of the developing network of insulating capacitance elements (C) [9, 13], indicating that the material undergoes a shear induced transition from a conducting state to an insulating state.

Fig. 4 illustrates the effect of shear on CNT concentrations of 0.15%, 0.3% and 0.75% by volume. At low shear rates the conductivity decreases slightly with increasing $\dot{\gamma}$, whereas above a critical value, it falls steeply. Evidently, a lower concentration CNT dispersion is substantially more susceptible to perturbation by flow. The overall character of the conductivity plots suggests a reverse-percolation transition where higher $\dot{\gamma}$ would correspond to a lower concentration of the conducting filler. In the case of φ = 0.15% by volume, σ_0 approaches the insulating limit of the PP matrix of about 10^{-8} S/m at $\dot{\gamma}$ above 6 s^{-1}. At these high shear rates, the conductivity data almost coincide with pure PP indicating that the material becomes a shear induced dielectric insulator. For the quiescent case we find that the characteristic steep rise in conductivity starts at φ of about 0.12% by volume. The applied shear field shifts the conductivity percolation condition for σ_0 to higher CNT content and shear also broadens the transition. These observations confirm our hypothesis that the sensitivity of the CNT network to a shear flow perturbation is greatest near the percolation transition
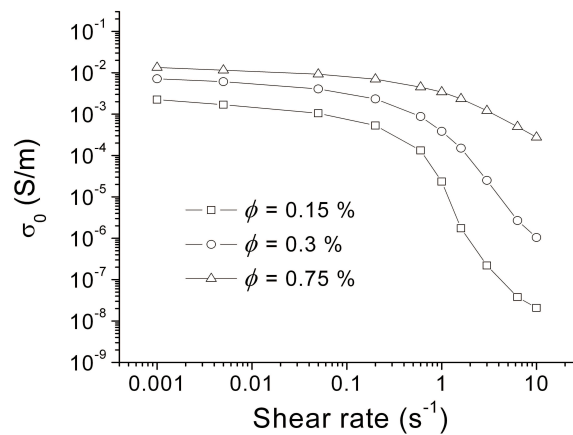

Fig. 4. Conductivity σ_0 as a function of shear rate.

where CNT only form a *weakly* interconnected network. The network becomes more robust when the CNT concentration is several times above the percolation threshold. We determined the conductivity percolation concentration (ϕ_c) as a function of shear rate by analyzing the data in Fig. 4 in terms of Generalized Effective Medium theory (GEM) percolation model [15, 16].

$$\sigma_0 = \sigma_a[(\phi - \phi_c)/(1 - \phi)]^t, \qquad (\phi > \phi_c), \tag{7a}$$

$$\sigma_0 = \sigma_i[(\phi_c)/(\phi_c - \phi)]^s, \qquad (\phi < \phi_c), \tag{7b}$$

where σ_0 is the measured conductivity, σ_a is the conductivity of additives (CNT), σ_i is the conductivity of the insulating matrix (PP), ϕ is the volume fraction of CNts in PP, ϕ_c is the critical percolation concentration, and t and s are the universal percolation exponents. We were able to fix the percolation exponent t governing the concentration dependence of σ_0 in the low shear rate regime to the theoretical value of $t = 2$ [12, 16] for all our data, but the value of the other exponent s had to be adjusted ($s \approx 1.3$ to 2.7) compared to the three-dimensional theoretical value of $s = 0.7$ [12, 16]. The resulting estimates of ϕ_c as a function of shear rate are shown in Fig. 5. For the quiescent case, we find that the ϕ_c is on the order of 0.12 vol. fraction %, while the applied shear field monotonically shifts ϕ_c to a higher CNT concentration. This trend is predicted by the geometrical percolation theory under the reasonable assumption that shear causes some alignment of the CNT, which is known to increase the geometrical percolation threshold in networks formed of overlapping extended particles [2, 17]. The influence of shear on the viscosity of dispersions of extended particles in fluids has been considered in several previous works and the shear dependence of the viscosity percolation was estimated in this context [17]. Thus, we may utilize the viscosity percolation threshold estimates to describe the shear rate dependence of ϕ_c:

$$\phi_c(\dot{\gamma}) = \phi_{co} + (\phi_{c\,\max} - \phi_{co})\frac{(\tau\dot{\gamma})^2}{1 + (\tau\dot{\gamma})^2}. \tag{8}$$

In Eq. 8 ϕ_{co} is the quiescent value of ϕ_c, the amplitude $\phi_{cmax} - \phi_{co} = \Delta\phi_c$ is the maximum change in ϕ_c induced by the flow, and τ is a flow relaxation time governing flow-induced particle orientation process. The value of τ is on the order of the structural relaxation time of an entangled polymer melt matrix. Specifically, the anisotropic particles are assumed to be initially dispersed isotropically for $\dot{\gamma} \to 0$ and the shift $\phi_{cmax} - \phi_{co}$ describes the effect of particle alignment along the shear field direction in the limit $\dot{\gamma} \to \infty$. The solid line in Fig. 5 shows a fit of the ϕ_c data to Eq. 8, where we obtain $\tau \approx 1$ s. The observation that ϕ_c increases with $\dot{\gamma}$ according to Eq. 8 supports our interpretation of the conductor-insulator transition as arising from the flow-induced alignment of the CNTs along the fluid flow direction. The maximum change in $\Delta\phi_c$ occurs for $\dot{\gamma}_c \approx 1/\tau \approx 1$ s^{-1}, which is consistent with τ being comparable to the structural relaxation time of the polymer matrix. A large part of this trend reflects the breaking down of the CNT network structure that forms through a combination of direct inter-tube attractive interactions, topological interactions between the tubes due strong excluded volume interactions that keep the tubes from passing through each other under flow and strong direct contact interactions arising from the physical impingement of these relatively rigid particles.
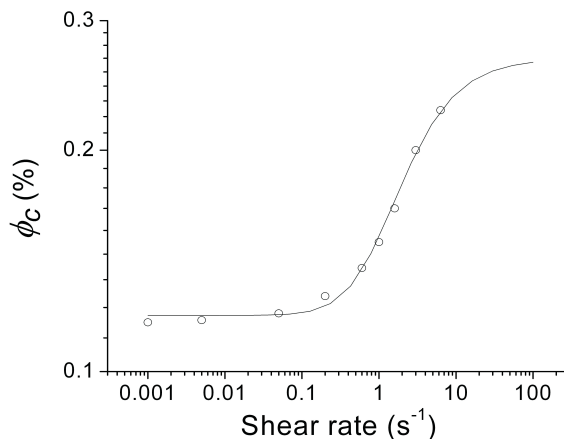
Fig. 5. Critical percolation concentration (ϕ_c) as a function of shear rate where circles s represent the calculated ϕ_c data while the solid line is a fit to Eq. (8).

4. CONCLUSION

Through precise complex conductivity measurements under mechanical shearing, we observed the conductor-insulator or 'percolation' transition in melt-mixed dispersions of multi-wall CNTs in polypropylene over a narrow range of CNT concentrations. The scaled conductivity for percolated networks ($\phi > \phi_c$) compares well with the universal trend showing power law behavior ($\sigma'(\omega)/\sigma_0 \sim \omega^n$). With increasing shear rate and decreasing CNT concentration, the exponent n decreases continuously, indicating that the fraction of resistive paths decreases with shearing in favor of the developing network of insulating elements. The shear-induced conductor-insulator transition has its origin in the shear rate dependence of the critical percolation concentration (ϕ_c), which increases with shear rate in accordance with our model for the shear-dependent percolation-threshold. According to this model, the quiescent value of ϕ_c is on the order of 0.12% by volume (0.36% by mass), while the structural relaxation time of the polymer matrix is about $\tau \approx 1$s. The observation that ϕ_c increases with $\dot{\gamma}$ according to Eq. 6 indicates that the $\dot{\gamma}$ field-induced alignment of the CNTs is along the fluid flow directions. Since ϕ_c and τ are universal parameters of the percolated network, Eq. 6 can be used as a predictive tool in analysis of shear induced behavior of other materials.

DISCLAIMER

Certain equipment, instruments or materials are identified in this paper in order to adequately specify the experimental details. Such identification does not imply recommendation by the NIST nor does it imply the materials are necessarily the best available for the purpose.

REFERENCES

1. Baughman R. H., Zakhidov A. A., De Heer W. A.: "Carbon Nanotubes-the Route Toward Applications". *Science*, vol. 297, 2002, pp. 787–792.
2. Moniruzaman M., Winey K I.: "Polymer Nanocomposites Containing Carbon Nanotubes". *Macromolecules*, vol. 39, 2006, pp. 5194–5205.
3. Simien D., Fagan J. A., Luo W., Douglas J. F., Migler K., Obrzut J.: "Influence of nanotube length on the optical and conductivity properties of thin single-wall carbon nanotube networks". *ACS NANO*, vol. 2 no. 9, 2008, pp. 1879–1884.
4. Kharchenko S. B., Douglas J. F., Obrzut J., Grulke E. A., Migler K. B.: "Flow-induced properties of nanotube-filledpolymer materials". *Nature. Mat.*, vol. 3, 2004, pp. 564–568.
5. Hilding J., Grulke E. A., Zhang Z. G., Lockwood F.: "Dispersion of Carbon Nanotubes in Liquids ". *J. Dispersion Sci. and Tech.*, vol. 24, 2003 pp. 1–41.
6. R. Andrews, D. Jacques, Qian D., Dickey E. C.: "Purification and structural annealing of multiwalled carbon nanotubes at graphitization temperatures". *Carbon*, 39, 1681 (2001).
7. Kashiwagi T., Grulke E. A., Hilding J., Groth K., Harris R., Butler K., Shields J. Kharchenko S. B., Douglas J.: "Thermal and flammability properties of polypropylene/carbon nanotube nanocomposites". *Polymer*, vol. 45, 2004 pp. 4227–4239.
8. Straley J. P.: "Critical exponents for the conductivity of random resistor lattices". *Phys. Rev.*, B vol. 15, 1977 pp. 5733–5737.
9. Clerc J. P, Giraud G., Laugier J. M., Luck J. M.: "The electrical conductivity of binary disordered systems, percolation clusters, fractals and related models". *Advances in Physics*, vol. 39, 1990, pp. 191–309.
10. Obrzut J., Douglas J. F., Kharchenko S. B., Migler K. B.: "Shear-induced conductor-insulator transition in melt-mixed polypropylene-carbon nanotube dispersions". *Phys Rev.*, B vol. 76, 2007, pp. 195420, 1–9.
11. Alig I.,Lellinger D., Dudkin S. M., Potschke P.: "Conductivity spectroscopy on melt processed polypropyleneemultiwalled carbon nanotube composites: Recovery after shear and crystallization". *Polymer*, vol. 48, 2007, pp. 1020–1029.
12. Dyre, J. C., Shroder, T. B.: "Universality of ac conduction in disordered solids". *Rev. Mod. Phys.*, vol. 72, 2000, pp. 873–892.
13. Hunt, A.G.: "AC hopping conduction: perspective from percolation theory". *Phil. Mag.*, vol. 81, 2001, pp. 875–913.
14. Pasveer, W. F., Bobbert, P. A., Michels, M. A. J.: "Universality of AC". *Phys. Rev.*, B 74, 165209 (2006).
15. McLachlan D. S., Blaszkiewicz M., Newnham R. E.: "Electrical Resistivity of Composites". *J. Am. Ceram. Soc.*, vol. 73, 1990, pp. 2187–2203.
16. McLachlan, D. S., Chiteme C., Park C., Wise K. E., Lowther S. E., Lillehel P. T., Siochi E. J., Harrison J. S.: "AC and DC percolative conductivity of single wall carbon nanotube polymer composites". *J. Polym. Sci.*, B vol. 43, 2005 pp. 3273–3297.
17. Douglas J. F., Garboczi E. J.: "Intrinsic Viscosity and the Polarizability of Particles Having a Wide Range of Shapes". *Adv. Chem. Phys.*, vol. 91, 1995, pp. 85–113.